Active Ankle – an Almost-Spherical Parallel Mechanism

Marc Simnofske[a], Shivesh Kumar[a], Bertold Bongardt[a], Frank Kirchner[ab]
{marc.simnofske, shivesh.kumar, bertold.bongardt, frank.kirchner}@dfki.de (MAIL) / +49·421·17845·4150 (FAX)

[a] DFKI GmbH, Robotics Innovation Center, Robert-Hooke-Str. 1, 28359 Bremen, Germany.
[b] Universität Bremen, Fachbereich Mathematik und Informatik, Arbeitsgruppe Robotik.

Abstract

Since parallel manipulators only provide restricted workspaces in comparison to their serial counterparts they cannot compete as versatile multi-purpose tools in flexible industrial setups. However, their superior properties in terms of stiffness, payload, speed, and acceleration often allow an advantageous application in more tailored use-cases. This paper lays out the concept of a novel parallel mechanism – called the ACTIVE ANKLE – which operates in an almost-spherical manner with three degrees of freedom. The text motivates the primarily intended application of the novel device as an ankle joint of a full-body exoskeleton. In addition, the paper discusses the design, the topology, results of a motion simulation, and a comparison with related mechanisms of the ACTIVE ANKLE.

Keywords: Mechanical Design; Parallel Manipulators; Spherical Mechanisms; Kinematic Analysis.

1 Introduction

A parallel manipulator (PM) is defined as a closed-loop mechanism in which the end-effector (mobile platform) is connected to the base by at least two independent kinematic chains [1]. On the contrary, a serial manipulator is defined as a mechanism in which the end effector is connected to the base by a single series of links and joints. In comparison to a serial mechanism, a parallel mechanism can offer higher stiffness, speed, accuracy and payload capacity, at the downside of a reduced workspace and a more complex geometry that needs careful analysis and control.

Due to the aforementioned advantages over serial manipulators, various parallel kinematic mechanisms were investigated and analyzed since the end of the 1980s in the fields of industrial automation and machine tools. However, both fields of application presume a large workspace. Hence, parallel kinematic mechanisms are quite inappropriate for these applications and only a few of them have been successfully commercialized. The DELTA robot [2] and its variants [3] probably represent the most popular class of PMs employed in industry.

In contrary to these industrial applications, in exoskeletons or physical man-machine interfaces, most joints require a limited range of motion because most of the human joints like the wrist or ankle are not able to fulfill a complete rotation movement. Hence, to protect the human body in an exoskeleton a physical limitation of joint movements is necessary. Thus, an exoskeleton based on serial kinematic chain does not guarantee enough safety because the software based joint limits may fail and hence additional mechanical end stops are required at each joint. The use of parallel manipulators in exoskeletons can not only reduce the moving masses but also their workspace limitation becomes an additional safety feature. The human body consists of several joints with three rotational movements which act like spherical joints, e.g. the wrist, ankle, hip and shoulder. In the literature, there exist only some parallel manipulators [4], [5], [6], [7] which can perform a spherical movement.

If the location of a point on the end-effector's lamina [8] of a PM remains constant, the device is called a spherical parallel manipulator (SPM). The AGILE EYE [4] and its improved variant AGILE WRIST [9] are prominent examples of SPMs with three degrees of freedom (DOF). The joint axes of this type of SPM are required to intersect in a single point. However, due to machining and assembling errors, it is difficult to achieve an accurate intersection of all joint axes. Misalignments may lead to increased tension and forces in the structure, and hence to a reduced service life of bearings or sometimes makes the complete system difficult to assemble. Moreover, the use of C-shaped links in the system prevents it from being used in high payload applications. Due to the kinematic layout that requires an exact intersection of all rotation axes, a high-precision manufacturing is indispensable for these SPMs [10].

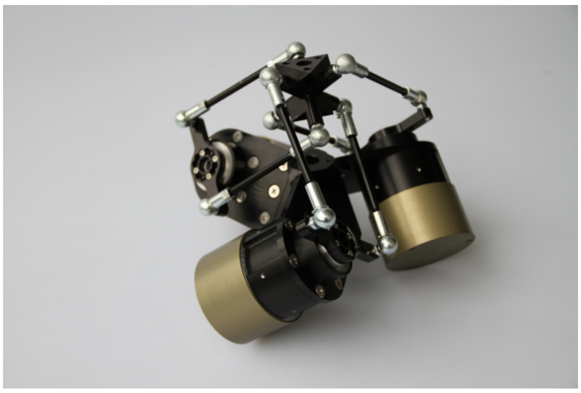

Figure 1: A built-up prototype of the ACTIVE ANKLE.

In this paper, a novel concept is introduced: due to the design of the mechanism ACTIVE ANKLE (see Figure 1), the constraint of moving the end-effector about an exact center (of rotation) in case of SPMs is relaxed to almost spherical motions that includes a shift of the end effector about a tolerated, small domain. Due to its simple and robust design, the presented almost-spherical parallel manipulator (ASPM), developed primarily for an ankle-joint in an exoskeleton, is estimated to have high potentials in other applications with small workspace requirements.

The paper is organized as follows: Section 2 presents the design and construction of the ASPM including its application scenario as an ACTIVE ANKLE joint, Section 3 presents the kinematic analysis and simulation of the ASPM using ADAMS and SIMULINK, Section 4 presents the comparison of this mechanism with other existing spherical devices in the literature and Section 5 concludes the paper.

2 Design and Construction

Several different classes of PMs exist for different applications. The type synthesis of PMs consists in finding all the possible types of PMs generating a specified motion pattern of the moving platform [11]. An overview of type synthesis of spatial parallel manipulators proposed by Frindt [12] is shown in Table 1.

The various possible leg configurations can be derived using the Kutzbach-Grübler formula. Table 1 describes the possibilities by using the relation between the desired degree of freedom of the parallel manipulator d, the number of kinematic chains k, and the sum of the joint DOF of each chain f. Each kinematic leg can be realized by a serial arrangement of links and joints or with closed loops. The latter comes with an inherent advantage of increased stiffness. For example, in the famous DELTA robot which has 3 DOF, each of its three legs is realized by a closed parallelogram (4S) mechanism which makes it a stiff positioning system. This is an inspiration for finding a novel parallel manipulator which can produce spherical movements while still keeping the topological arrangement of DELTA robot.

The layout of the novel ASPM is depicted in Figure 2: the device features three rotative actuators fixed to the base. Each of the motors drives a spatial quadrilateral consisting of a symmetric crank, two rods, and a line segment on the mobile platform. The three line segments mutually intersect orthogonally and together form a spatial cross on the end-effector link.

A crucial feature of the mechanism's design is the stress distribution among the structure: the six rods that transmit the forces from the cranks to the platform are only loaded with forces along their axes, due to the spherical joints at their ends. For this uniaxial stress conditions semi-finished products like carbon fiber tubes could be used for a lightweight design. Also, it must be noted that due to redundant degrees of freedom, the replacement of one spherical joint by a universal joint at each bar is possible.

Further advantages of the design include the large amount of same parts of simple shapes, permitting a low-cost construction, and the robustness against production inaccuracies due to the design simplicity. The ASPM was developed and patented by the Robotics Innovation Center (RIC), DFKI GmbH [13].

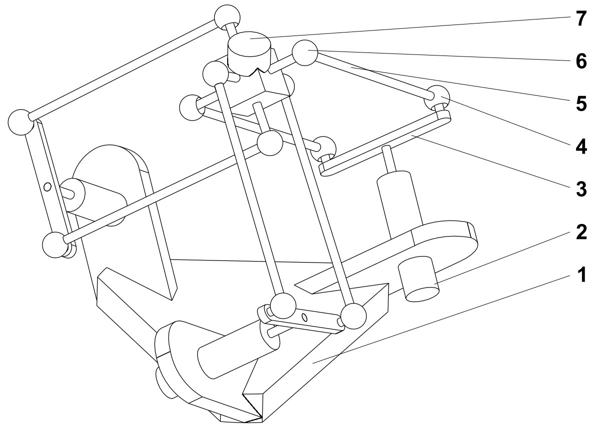

Figure 2: Sketch of the ACTIVE ANKLE [13] including (1) base, (2) rotative actuator, (3) crank, (4 & 6) ball and socket joints, (5) rod, (7) end-effector.

The topology of the mechanism is depicted in Figure 3. The $n = 11$ links L_i are enumerated as L_{01}, L_{12}, L_{13}, L_{14}, L_{23}, L_{32}, L_{33}, L_{43}, L_{52}, L_{53}, and L_{63}. The $m = 15$ joints $J_{i,j}$ are distinguished using double indices, as indicated in Figure 3. The number of independent loops of the ACTIVE ANKLE is computed with $c = m - n + 1 = 11 - 15 + 1 = 5$. For computing the general mobility number by means of the Kutzbach-Grübler formula

$$d_s(\mathcal{M}) = s \cdot (n - m - 1) + f = s \cdot (-c) + f \ ,$$

the total number of freedoms $f = \sum_{ij} f_{ij}$ needs to be determined: three rotative joints, six spherical joints, and six universal joints, result in $f = 3 \cdot 1 + 6 \cdot 3 + 6 \cdot 2 = 3 + 18 + 12 = 33$, yielding a general mobility of

$$d_s(\mathcal{M}) = 6 \cdot (11 - 15 + 1) + 33 = 3 \ .$$

Since the device is *almost* a spherical device, the motion parameter s equals six (spatial) and not three (spherical).

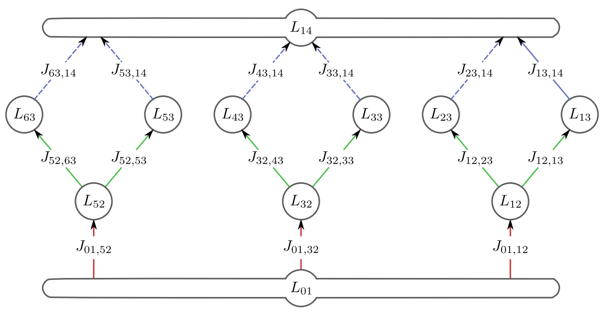

Figure 3: Link graph of the parallel manipulator ACTIVE ANKLE, including $n = 11$ links and $m = 15$ joints.

The ACTIVE ANKLE is developed for an innovative and mobile full-body exoskeleton for robot-assisted rehabilitation of neurological diseases. The exoskeleton is intended mainly for stroke patients with one-sided arm

	$d=2$	$d=3$	$d=4$	$d=5$	$d=6$
$k=2$	2 6, 3 5, 4 4	3 6, 4 5	4 6, 5 5	5 6	6 6
$k=3$	–	3 6 6, 4 5 6, 5 5 5	4 6 6, 5 5 6	5 6 6	6 6 6
$k=4$	–	–	4 6 6 6, 5 5 6 6	5 6 6 6	6 6 6 6
$k=5$	–	–	–	5 6 6 6 6	6 6 6 6 6
$k=6$	–	–	–	–	6 6 6 6 6 6

Table 1: Overview of spatial parallel manipulators with general mobility d and their distributions of degrees of freedom to k kinematic chains (legs) connecting base and mobile platform. Sketch in accordance to [12]. The topological type of the almost-spherical ACTIVE ANKLE is highlighted.

paralysis to support the movements of an affected arm during robot assisted therapies. A full body exoskeleton is necessary to avoid that the patient has to carry the load of the upper body exoskeleton. Figure 4 shows a CAD model of the ACTIVE ANKLE arrangement in the foot unit. The exoskeleton is designed in the way that during walking the ACTIVE ANKLE has to fulfill a motion range of 20° approximately back and forth. In simple case, while standing on one leg it has to carry the load of the full- body exoskeleton (initial estimation of weight: 30 kg) and the concerned human arm.

For sake of a high modularity, specific motor units, designed in the iStruct project [14], have been adapted for the ACTIVE ANKLE. Each actuator (Figure 5) is realized by a brushless DC-motor coupled with a harmonic drive gear and allows a nominal torque of 28 Nm and a speed of 300 RPM at the output with a weight of 392 g.

For achieving an autonomous, fully functional unit, all control and power electronics are integrated in the actuator module (Figure 5). Thus, the cable loom is reduced to cables for 48-V power supply and communication wires for two full duplex Low-Voltage Differential Signaling (LVDS) point-to-point connections between the joints.

The electronics were developed within the space climber project [15] and further improved continuously. The basic control sensors on the actuator are two iC-MU off-axis nonius encoders with integrated hall sensors of 12-bit resolution. One of the sensors is located directly on the rotor. The decision to use its signals for the speed controller yields a simple and robust setup. The core electronic component which undertakes tasks as control of current, speed, and position, real-time logging of sensor data, as well as communication with other actuators and the central processing unit has been created from a Xilinx Spartan-3 FPGA [15].

A multibody analysis followed by an FEM analysis has been performed to check the deformation of the critical parts like rods and cranks under desired loads (Figure 6). A force resulting due to the weight of the exoskeleton and human arm was applied to the end effector and the forces in the spherical joints were measured. In zero configuration, this force – equivalent to 350 N when perpendicular to the end effector – leads to a reaction force of approximately 100 N in each spherical joint. The selected ball and socket joints are designed for a maximum axial tensile force of 600 N in housing axis and a pivot angle of maximum of $\pm 25°$. The same magnitude of force occurs in the rods and this force has been found to be less than the buckling force of the rods (i.e. 2120 N). Thus, it is ensured that the mechanism resists from buckling in all possible configuration.

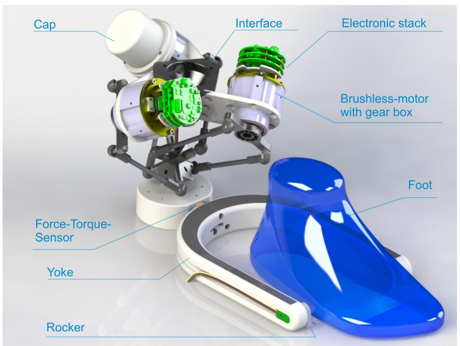

Figure 4: ACTIVE ANKLE integrated into the foot unit of an exoskeleton.

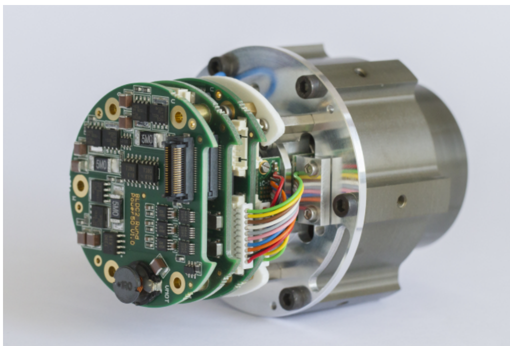

Figure 5: One of the three actuation modules of ACTIVE ANKLE, including the motor and electronics.

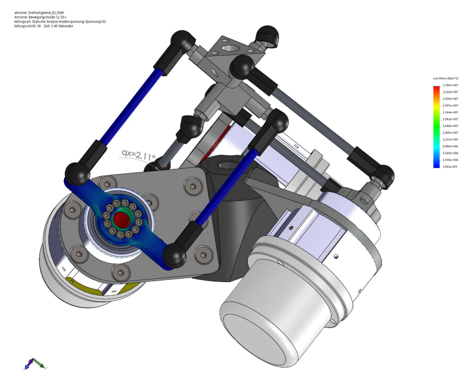

Figure 6: FEM analysis of the ACTIVE ANKLE after a multibody analysis.

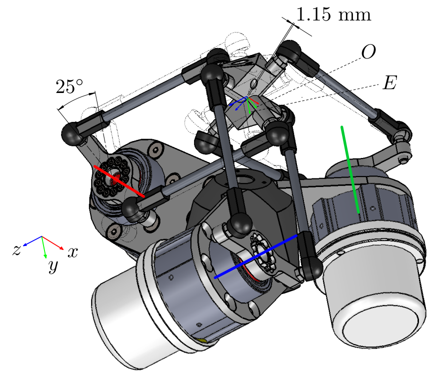

Figure 7: ACTIVE ANKLE with origin O and the displaced end-effector frame E for q_{12} set to 25°.

3 Kinematic Analysis and Simulation

To analyze the behavior of the 3-DOF ACTIVE ANKLE mechanism, a kinematic simulation using ADAMS is performed. It is recalled that the ball and socket joints used in the construction of this mechanism have a motion range of $\pm 25° \approxeq \pm 0.4363$ rad. Thus, the maximum possible motion range for the three rotative joints ($J_{01,12}$, $J_{01,32}$, and $J_{01,52}$) lays between $-25°$ and $+25°$. Since ACTIVE ANKLE is a spatial mechanism which behaves in an almost spherical manner, the output motion of the end effector consists of primarily rotation and small translations. Let us consider a global coordinate system (O) attached to the ground at the center of the end effector (when in zero configuration) such that its x axis is aligned with the joint axis of $J_{01,12}$, y axis is aligned with joint axis of $J_{01,32}$ and z axis is aligned with joint axis of $J_{01,52}$. To measure the position and orientation of the end effector, let us consider an end-effector coordinate system (E) attached with the end-effector which is coincident with global coordinate system (O) only when the manipulator is in its zero configuration. The rotation between these two frames (i.e. E and O) is measured in terms of roll, pitch, and yaw angles and the translation of the end effector is measured by the coordinates of frame E, the point $\boldsymbol{e} = (e_x, e_y, e_z)^T$ w.r.t. the global coordinate system O. Figure 7 shows the position of frames E and O on the ASPM when q_{12} is set to 25°. The length of the six rods is 10 cm, length of the three rotative cranks is 7 cm and length of the three orthogonal line segments constituting the end effector is 7 cm. Three motion simulation cases are presented in this section to demonstrate the almost spherical behavior of this mechanism.

Firstly, a sinusoidal joint motion trajectory with amplitude of 0.4363 rad and frequency 2π rad/s has been provided to the rotative joint aligned with the global x axis (i.e. $J_{01,12}$) while the other two joint angles are set to zero. The simulation time is set to 1 s with 100 time steps. The input and output rotative motions have been compared in Figure 8. In this case, it is interesting to observe that roll angle of the end effector is equal to input joint angle $J_{01,12}$. Also, it is observed that a translational motion (with peaks of $e_x = 1.1542$ mm, $e_y = 0.0067$ mm, $e_z = 0.0067$ mm) primarily in the direction of x axis is induced which is indeed very small in comparison to the size of the mechanism. The small translational motion of the end-effector for the given input motion has been plotted w.r.t. time in Figure 9. If the input rotative motion is about y or z axis while keeping the other two zero, an equivalent output rotative motion in terms of pitch and yaw is observed coupled with small and primary translational shifts along y or z axis.

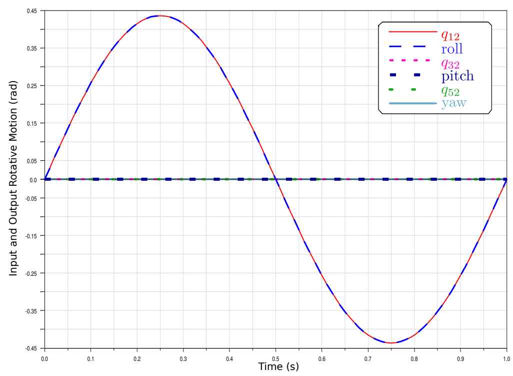

Figure 8: Plots of an exemplary input motion, with $q_{12} = 0.4363 \cdot \sin(2\pi \cdot t)$ and $q_{32} = q_{52} = 0$, and of the corresponding rotative part of the output motion of the ACTIVE ANKLE.

A second interesting simulation case is when a ramp signal of slope 0.4363 rad is provided at all input rotative joints. The simulation time is set to 1 s with 100 time steps like in previous case. In Figure 10, it can be observed that all three input motions has now an effect on the end effector coordinates ($e_x = e_y = e_z = 0.5058$ mm at $t = 1$ s). The net translation of the end effector is much smaller in comparison to previous simulation.

Lastly, to analyze the workspace shape of the ACTIVE ANKLE, a co-simulation using ADAMS and SIMULINK has been performed within a motion range of $\pm\pi/11$ radian for each of the three input joints, $J_{01,12}$, $J_{01,32}$, and $J_{01,52}$. The translational part of the output motion of the end-effector is shown in Figure 11. The rotational part

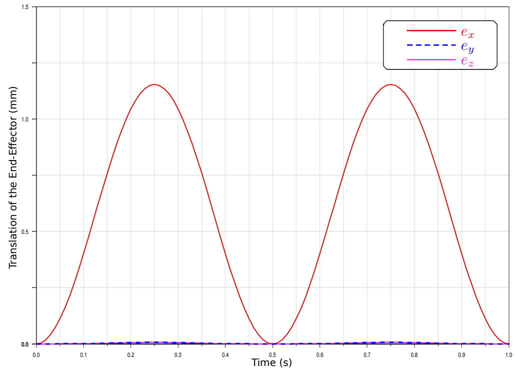

Figure 9: Translational motion of the end effector in case of sinusoidal input at one joint.

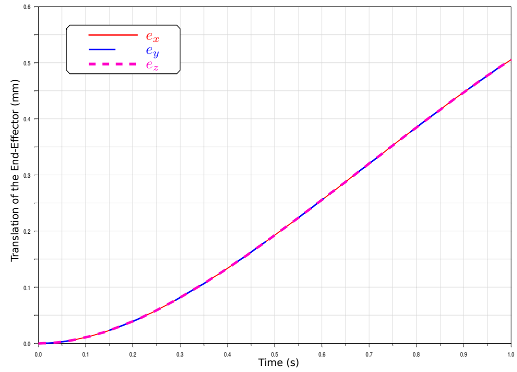

Figure 10: Small translational motion of the end effector in case of ramp input at all joints.

of the output motion is expressed in roll, pitch, and yaw in comparison to the input of the three active joints in Figure 12. The two figures demonstrate that the device achieves three DOF in the rotational workspace while the end-effector only undergoes small translational displacements for the simulated input configurations.

4 Discussion

From a practical perspective, the novel ACTIVE ANKLE is estimated to increase robustness and decrease costs in applications that require almost spherical movements with high stiffness. For example, the novel device could be used to create joints within exoskeletons which interact with the motions of human operators, that are based on highly complex motion patterns and not on 'perfectly-spherical symmetries'. From a theoretical perspective, the almost-spherical ACTIVE ANKLE is presented in contrast with spherical devices in Table 2.

Mechanism	Ref.	Links n	Joints m	Loops c
RRR / Cardan	[16]	4	3 (6)	0 (3)
Agile Eye / Wrist	[4]	8	9	2
AsySPM	[5]	11	13	3
CamSPM3	[6]	8	10	4
Hexasphere	[7]	14	19	6
Active Ankle	[13]	11	15	5

Table 2: A comparison of mechanisms, in terms of their members, links n, joints m, and number of independent loops $c = m - n + 1$.

The simplest spherical device can be a serial RRR chain or the Cardan mechanism [16] with three with intersecting axes. Due to its construction, it lacks the stiffness which its parallel counterparts can offer. AGILE EYE and its variants are good examples of Spherical Parallel Manipulators (SPMs) for high speed orientation tasks with low payload like a camera. But they require high manufacturing and assembly accuracies for the intersection of all rotative axes. A small misalignment in the assembly can lead to unnecessary tensions in the links which decreases the life of the structural components like rotative bearings. Also, the use of C-shaped links in their design makes them unsuitable for high payload applications. Asymmetrical Spherical Parallel Manipulator ASYSPM [5] promises an unlimited torsional motion capability but involves the use of large number of different parts (including two C-shaped links) in its assembly due to its asymmetrical leg configuration. 3-PSS manipulator (abbreviated as CAMSPM3 in Table 2) has been designed for similar applications as AGILE EYE and avoids the use of C-shaped links but is possible only because of a presence of passive leg. HEXASPHERE [7] is a highly stiff SPM which uses straight rods but is redundantly actuated with six motors to achieve only three DOF.

ACTIVE ANKLE in comparison to all these mechanisms offers significantly better stiffness (exception HEXASPHERE), a simple and elegant design, and robustness against assembling errors. At the same time it is very suitable for high payload applications which most SPMs in the literature cannot guarantee. Moreover, the motors do not need any active torques to carry the external load if the load is acting in direction of torsional rotation axis of the end-effector. It must be noted that the ACTIVE ANKLE behaves in an almost-spherical manner and its rotation movements are always coupled with small translation movements (1-2 mm for the presented version) which can be neglected for several practical applications. Still, the ASPM ACTIVE ANKLE can also be integrated as a submechanism into a larger manipulator for obtaining precise six DOF motions if the constrained translations of the ASPM are compensated by the previous and / or the subsequent joints of the overall device.

5 Conclusion

This paper presents the ACTIVE ANKLE, a novel parallel manipulator with mobility three that moves in an almost spherical manner. The design considerations, specifications, kinematic analysis and simulation of this mechanism, together with its comparison to existing spherical mechanisms are presented that unveil its distinctive features and suitability as an ankle joint in the exoskeleton. In the future, scaled variants of this design will be

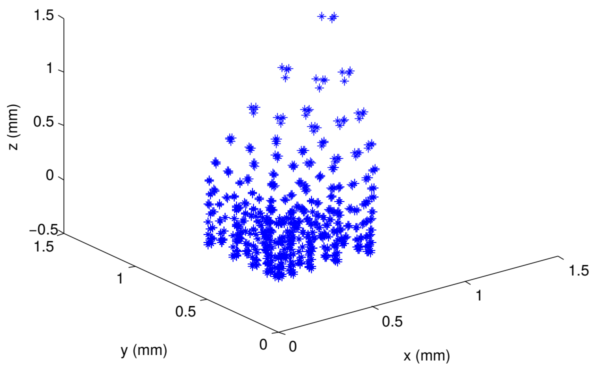

Figure 11: Translational workspace, constrained to a small domain.

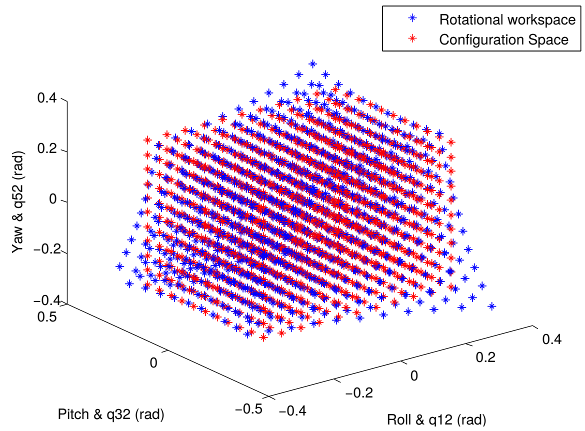

Figure 12: Configuration space and rotational workspace (roll, pitch, yaw).

produced for meeting the requirements of other spherical joints in exoskeleton for example, hip or shoulder. Furthermore, the ASPM developed will be tested as an almost-spherical wrist joint mounted on regional manipulator with three degrees of freedom to achieve six DOF in task space. Finally, it is planned to present analytical inverse kinematics solutions of the ACTIVE ANKLE together with workspace characterizations in a prospective publication.

Acknowledgement

This work was performed within the framework of RECUPERA-Reha project at Robotics Innovation Center, DFKI GmbH, Bremen, Germany. This project is funded by the German Aerospace Center (DLR) e.V. with federal funds from the Federal Ministry of Education and Research (BMBF) in accordance with the parliamentary resolution of the German Parliament, grant no. 01IM14006A.

References

[1] J. P. Merlet. “Parallel manipulators: state of the art and perspectives”. In: *Advanced Robotics* (1993).

[2] R. Clavel. “Conception d’un robot parallèle rapide à 4 degrés de liberté”. PhD thesis. EPFL Lausanne, 1991.

[3] J. Brinker and B. Corves. “A Survey on Parallel Robots with Delta-Like Architecture”. In: *IFToMM World Congress*. 2015.

[4] C. Gosselin, E. St-Pierre, and M. Gagne. “On the development of the agile eye: mechanical design, control issues and experimentation”. In: *IEEE Robotics and Automation Society Magazine* 3.4 (1996).

[5] G. Wu, S. Caro, and J. Wang. “Design and transmission analysis of an asymmetrical spherical parallel manipulator”. In: *Mechanism and Machine Theory* 94 (2015), pages 119–131.

[6] T. Villgrattner, E. Schneider, P. Andersch, and H. Ulbrich. “Compact High Dynamic 3 DoF Camera Orientation System: Development and Control”. In: *Journal of System Design and Dynamics* 5.5 (2011), pages 819–828.

[7] M. Valasek, J. Zicha, M. Karasek, and R. Hudec. “Hexasphere – Redundantly Actuated Parallel Spherical Mechanism as a New Concept of Agile Telescope”. In: *Advances in Astronomy* (2010).

[8] J. K. Davidson, K. H. Hunt, and G. R. Pennock. *Robots and Screw Theory: Applications of Kinematics and Statics to Robotics*. Oxford University Press, 2004.

[9] A. Niyetkaliyev and A. Shintemirov. “An approach for obtaining unique kinematic solutions of a spherical parallel manipulator”. In: *IEEE/ASME International Conference on Advanced Intelligent Mechatronics (AIM)*. 2014, pages 1355–1360.

[10] K. Al-Widyan, X. Q. Ma, and J. Angeles. “The robust design of parallel spherical robots”. In: *Mechanism and Machine Theory* 46.3 (2011), pages 335–343.

[11] Kong and Gosselin. *Type Synthesis of Parallel Mechanisms*. Springer tracts in advanced robotics, 2007.

[12] M. Frindt. “Modulbasierte Synthese von Parallelstrukturen für Maschinen in der Produktionstechnik”. PhD thesis. Technical University of Braunschweig, 2001.

[13] M. Simnofske. *Ausrichtungsvorrichtung zum Ausrichten einer Plattform in drei rotatorischen Freiheiten*. Patent application, DE102013018034A1. 2015.

[14] D. Kuehn, F. Bernhard, A. Burchardt, M. Schilling, T. Stark, M. Zenzes, and F. Kirchner. “Distributed Computation in a Quadrupedal Robotic System”. In: *International Journal of Advanced Robotic Systems, InTechOpen, volume o.A.* (2014).

[15] S. Bartsch, T. Birnschein, M. Langosz, J. Hilljegerdes, D. Kuehn, and F. Kirchner. “Development of the six-legged walking and climbing robot SpaceClimber”. In: *Journal of Field Robotics, Wiley Subscription Services, Volume 29, Issue 3, Special Issue on Space Robotics, number Part 1, pages 506-532* (June 2012).

[16] R. K. G. Temple. “The Cardan suspension”. In: *The UNESCO Courier* (1988).